Proceedings of the Estonian Academy of Sciences,
2014, **63**, 4, 404–416
doi: 10.3176/proc.2014.4.06
Available online at www.eap.ee/proceedings

PHYSICS

Spectral aerosol optical depth prediction by some broadband models. Validation with AERONET observations

Martin Kannel[a*], Hanno Ohvril[a], Oleg Okulov[b], Kaidi Kattai[a], and Lennart Neiman[a]

[a] Laboratory of Atmospheric Physics, Institute of Physics, University of Tartu, Ülikooli 18, 50090 Tartu, Estonia
[b] Estonian Environment Agency, Mustamäe tee 33, 10616 Tallinn, Estonia

Received 4 November 2013, revised 3 February 2014, accepted 5 February 2014, available online 20 November 2014

Abstract. A comprehensive investigation on the performance of aerosol optical depth at 500 nm (AOD500) predictions using broadband physical and statistical models is detailed here. Seven simple models and one more complicated model were selected. A special database with more than 26 000 broadband (direct solar beam) and spectral (AODλ) instantaneous observations at clear solar disc during 10 years (2002–2011) at Tõravere (Estonia) was compiled for the intercomparison. The database allows analysing the variability and climatological behaviour of several column parameters: coefficient of broadband transparency, precipitable water, AOD500, and the Ångström wavelength exponent (α). A statistical AOD500 model is finally recommended. It uses only two input parameters: coefficient of column broadband transparency and precipitable water. Two models from the set enabled variation of Ångström α. However, consideration of a priori known instantaneous α values did not improve predictions.

Key words: aerosol column optical properties, AERONET, column broadband transparency, Ångström exponent.

1. INTRODUCTION

Aerosol optical depth, AODλ, is a central parameter for the description of column aerosol content and column optical properties, including the rate of atmospheric turbidity. From the 1990s, after the start of the US NASA programmes AERONET, TerraMODIS, and AquaMODIS, this parameter became available and very popular (Holben et al., 1998; Toledano et al., 2007). However, in order to obtain a more capacious temporal and spatial overview of aerosol distribution, especially for retrospective (backward) extrapolation of AODλ time series to pre-1990 years when the photometric network was sparse, it is necessary to use alternative methods for calculation. There are also two other reasons for AODλ proxy, mainly broadband calculations: (1) quality inspection of recently measured AODλ time series, although by a modern solar photometer, because when the recorded values seem too large (overestimated for a certain period), a doubt always arises about an undesirable object (insect, spider's thread, trash, etc.) dwelling on or inside the instrument's tube; and (2) a quick AODλ estimation for correcting satellite remotely sensed data for regions or moments where/when spectral solar observations are not available but broadband ones are.

Several AODλ broadband models can be found from an extensive literature survey. The high-performance models are laborious for processing large amounts of data or they require either special or very accurate input quantities. However, there are other models which, especially for physical climatology, allow easy programming with no need of ancillary meteorological input data. Continuing activity in the development and modification of simple broadband models indicates that such approaches do correspond to practical needs.

In general, there are three main input parameters for simple AODλ models. One describes column attenuation of the broadband direct solar beam, e.g. broadband transmittance (τ_m), Bouguer coefficient of column

* Corresponding author, martin.kannel@ut.ee

transparency (p_m), column broadband optical depth (δ_m), Linke turbidity factor ($T_{\mathrm{L},m}$), which all are equal, linked by the well-known Bouguer–Lambert exponential law:

$$S_m = S_0\tau_m = S_0 e^{-m\delta_m} = S_0 p_m^m = S_0 e^{-m\delta_{\mathrm{CDA},m}T_{\mathrm{L},m}}. \quad (1)$$

Here S_m is the measured broadband irradiance at optical mass m; S_0 is the extraterrestrial broadband solar irradiance at the actual Sun–Earth distance, its average value, the "solar constant", is 1.367 kW m^{-2} (Lenoble, 1993); and $\delta_{\mathrm{CDA},m}$ is the optical depth of an ideal, i.e. clean and dry atmosphere (CDA).

To eliminate the Forbes effect, inherent to column broadband optical characteristics, the generally accepted practice is to reduce them from the actual optical air mass m to a standard air mass, mainly to $m = 2$ (solar elevation $h \approx 30°$). As to possible processes of reduction, it seems to us that quite successful methods have been developed in regard to the Bouguer coefficient p_m (Ohvril et al., 1999, 2009). For this reason, p_2 is the input parameter of several models in this study.

A second input parameter to simple models is column humidity (water vapour content). Its unit, *mass per unit area*, is in practice usually given as the thickness of the layer of liquid water: 1 mm corresponds to 1 kg m^{-2} and 1 cm to 1 g cm^{-2}.

A third parameter, the Ångström wavelength exponent, α, is closely linked to the size distribution of aerosol particles, provided that the size distribution, in part, follows a power law (Liou, 2002). However, the column aerosol particles are in permanent change, expressing deviations from the power law. Hence the wavelength exponent is actually a very unstable parameter, which has different values for different parts of the solar spectrum. As it is poorly correlated with AODλ, its use in atmospheric optical models is questionable.

The present work aims at validation of seven simple broadband models and one more complicated model for AODλ calculations.

Five simple models (M1, M2, M2a, M2b, and M2c) were developed in Moscow during 1991–2013, and two in Tartu (T1, T2) during 2007–2012. The most complicated model (G1) is Gueymard's parameterization from 1998, based on his known SMARTS2 code, and it allows considering numerous column parameters. The set of the used models (including references) will be described in detail in Section 2.

All models were tested against AOD500 reference values obtained by an AERONET photometer at Tõravere, Estonia, located in the territory of the Tartu-Tõravere Meteorological Station during 10 years, 2002–2011. The station (58.26°N, 26.46°E, 70 m ASL), is included into the Baseline Surface Radiation Network (Kallis et al., 2005).

Simultaneous registration of both spectral and broadband irradiances provided an opportunity to create a joint, integrated database for AODλ together with the Ångström exponent and broadband parameters of atmospheric transparency and turbidity. The joint database includes 26 091 spectral–broadband solar direct irradiance and surface water vapour pressure observations covering all months except December.

Although the AERONET observations, besides AODλ, give also values of precipitable water, W, we have considered that the input values for the models should be independent in regard to a reference instrument. For that, precipitable water was evaluated using surface water vapour pressure, e_0 (Okulov et al., 2002; Okulov and Ohvril, 2010).

2. A REVIEW OF THE USED BROADBAND MODELS

A quick review of the used broadband models together with their inputs and outputs can be obtained from Table 1.

2.1. Models M1 and M2

The models were developed in the Meteorological Observatory of the Moscow State University (Tarasova and Yarkho, 1991a, 1991b). Model M1 consists of 13 formulas; it is somewhat general and unique because it allows varying the Ångström wavelength exponent, α. Model M2 is a simplified version of M1, where the Ångström exponent has a fixed value, $\alpha = 1$. Model M2 is expressed by only one formula

$$\mathrm{AOD550} = \frac{\ln S_m - \left(0.189W^{-0.183} + \dfrac{0.880W^{-0.009} - 1}{\sin h}\right)}{0.813W^{-0.002} - 1 + \dfrac{0.435W^{-0.0321} - 1}{\sin h}}, \quad (2)$$

where h is solar elevation and W zenith precipitable water in centimetres.

Model M2 was widely used for monitoring aerosol turbidity in the Russian territory (Abakumova and Gorbarenko, 2008). Routine registration of broadband direct solar irradiance has been performed in Moscow since 1955. Before the development of models M1 and M2 in 1991, there was one summer, in 1972, when the region around Moscow was affected by extensive forest and peat fires, but in that summer the capabilities to check broadband calculations of AODλ by reference spectral instruments were limited. A solar-sky AERONET Cimel photometer was deployed in Moscow for measuring AODλ as early as in 2001. The next,

Table 1. List of the considered broadband AODλ models. Possible inputs: h – solar elevation; S_m – broadband direct solar irradiance; p_2 – broadband (integral) Bouguer coefficient of column transparency for optical air mass $m = 2$; W – precipitable water; α – Ångström wavelength exponent; O_3 – column ozone content; NO_2 – column nitrogen dioxide content

Model	Reference	Input	Number of formulas	Output	Correction of prediction
M1	Tarasova and Yarkho, 1991a, 1991b	h, S_m, W, α, $O_3 = 300$ DU	13	AOD550	Not used
M2	Abakumova and Gorbarenko, 2008	h, S_m, W, $\alpha = 1$, $O_3 = 300$ DU	1	AOD550	Not used
M2a	Chubarova, 2005	h, S_m, W, $\alpha = 1$, $O_3 = 300$ DU	2	AOD500	For AOD500 > 0.4
M2b	Chubarova, 2005	h, S_m, W, $\alpha = 1$, $O_3 = 300$ DU	2	AOD500	For AOD500 ≥ 0.063
M2c	Gorbarenko and Rublev, 2013	h, S_m, W, $\alpha = 1$, $O_3 = 300$ DU	2	AOD550	Depends on solar elevation
G1	Gueymard, 1998	h, S_m, W, $\alpha = 1.3$, O_3, NO_2	>30	AOD1000	Not used
T1	Kannel, 2007; Kannel et al., 2007	p_2, W, α, $O_3 = 300$ DU	1	AOD500	Not used
T2	Kannel et al., 2012	p_2, W	2	AOD500	Not used

extremely dry summer of 2002 favoured huge fires around Moscow and the city was filled with smoke (the CIMEL photometer is located near the main building of the university, in the territory of the botanic garden). Prediction of AODλ under the conditions with a large amount of smoke aerosols (in summer 2002) revealed the fact that model M2 gives lower values at very turbid air in comparison to AERONET simultaneous observations.

The main reason for the underestimation of AODλ at high turbidities by the broadband models is that the models consider only a "true" narrow solar direct beam, exactly from the solar disc with its mean angular diameter of about 32 arc minutes. Actually the opening angles of older broadband instruments, but still in use for homogeneity of multidecadal time series, have considerably wider apertures reaching up to 10°. For example, the Kipp & Zonen Linke–Feussner actinometer has an aperture of 10.2° (Gueymard, 1998; Garg and Prakash, 2006). The AT-50 actinometers, continuously in use in actinometric networks in the territory of the former USSR, have the full field of view, FOV = 10°.

Although the FOV of most current pyrheliometers is smaller (e.g. for the Eppley Laboratory Inc. normal incidence pyrheliometers (NIP) the FOV = 5.7°), the measured direct beam is anyway increased by undesirable diffuse irradiance intercepted by a broadband instrument (Gueymard, 1998; Carlund et al., 2003).

The magnitude of this increase is greater at low solar elevation and heavy aerosol loading, and also in cases of large aerosol particles such as maritime aerosol, biological aerosol, desert or ground dust, etc. In cases of small particles (e.g. almost pure molecular scattering in a clear atmosphere after a rain) circumsolar radiation is weaker. According to calculations made by Gueymard (1998) for FOV = 10.2°, the circumsolar magnification factor can reach 35% in regard to the true direct irradiance. Increased artificial values of the observed broadband direct beam, S_m, lead to underestimation of the modelled AODλ. The artificial increase in readings of modern spectral photometric observations is decreased due to the smaller aperture (e.g. for the CIMEL-318 radiometer, the FOV = 1.2°).

2.2. Model M2a

Analysis of data from a smoky summer of 2002 when AERONET observations in Moscow were already available, led to a conclusion that a better match between predicted and observed values at $AOD500^* > 0.4$ can be achieved by substitution of initially predicted $AOD500^*$ with its increased counterpart, AOD500 (Chubarova, 2005):

$$AOD500 = 1.301 \times (AOD500^*)^{1.095}. \quad (3)$$

The correction from $AOD500^* = 0.4$ towards bigger values increases the initially predicted $AOD500^*$ but also leads to an artificial discard of corrected aerosol optical depths in a range of $0.4 < AOD500 < 0.477$, which is a secondary visual defect rather than a functional imperfection. Application of model M2 together with the correction for $AOD500^* > 0.4$ is further denoted by M2a.

The third catastrophically dry and hot summer with flaming and smoldering wildfires around Moscow occurred in 2010. In contrast to previous smoky periods, in 1972 and 2002, the summer of 2010 was characterized by higher aerosol optical depths, reaching even a value of $AOD500 = 4.6$. In a review on radiation

monitoring of all three smoky summers Chubarova et al. (2011a, 2011b) recommended implementation of correction by Eq. (3) from $AOD500^* = 0.5$ onward, which means an absence of corrected AOD500 even in a larger range, 0.5–0.609.

2.3. Model M2b

However, in massive data processing, generation of a permanent empty zone for corrected AOD500 values is not desirable. On the other hand, for low $AOD500^*$ values correction by Eq. (3) is not significant. Moreover, below a certain value, $AOD500^* \le 0.062$, the implementation of Eq. (3) will lead instead of $AOD500^*$ enlargement to its reduction. For example, inserting $AOD500^* = 0.025$ into Eq. (3) one obtains $AOD500 = 0.023$. In such cases the *correction factor*, *CF*,

$$CF = \frac{\mathrm{AOD500}}{\mathrm{AOD500}^*} \tag{4}$$

obtains values <1.0. Use of Eq. (3) only for $AOD500^* \ge 0.063$ ($CF \ge 1$) avoids appearance of an empty zone for corrected AOD500 and secures a smooth correction. The use of Eqs (2) and (3) together with a condition for $AOD500^* \ge 0.063$ only is further denoted by M2b.

2.4. Model M2c

Recently Gorbarenko and Rublev (2013) reported about using a solar elevation-dependent correction of $AOD500^*$. Assuming continental aerosols with a fixed Ångström exponent, $\alpha = 1$, they derived a correction algorithm:

$$\mathrm{AOD550} = (\mathrm{AOD550}^*)\left[0.9 + \frac{(\mathrm{AOD550}^*)^{\frac{0.7}{0.75\sin h + 0.125}}}{5}\right], \tag{5}$$

which they further applied for $AOD550^* > 0.5$. Because $AOD500^* = 1.1 \times AOD550^*$, the next algorithm for 500 nm can be obtained:

$$\mathrm{AOD500} = \left(\frac{\mathrm{AOD500}^*}{1.1}\right)\left[0.9 + 0.2\left(\frac{\mathrm{AOD500}^*}{1.1}\right)^{\frac{0.7}{0.75\sin h + 0.125}}\right]. \tag{6}$$

However, the two last formulas reduce the first calculated AOD^* for cleaner air also (i.e. in cases of low aerosol content) like the use of correction by Eq. (3). For example, in case of $AOD500^* = 0.36$ and $\sin h = 0.5$, Eq. (6) gives $AOD500 = 0.34$.

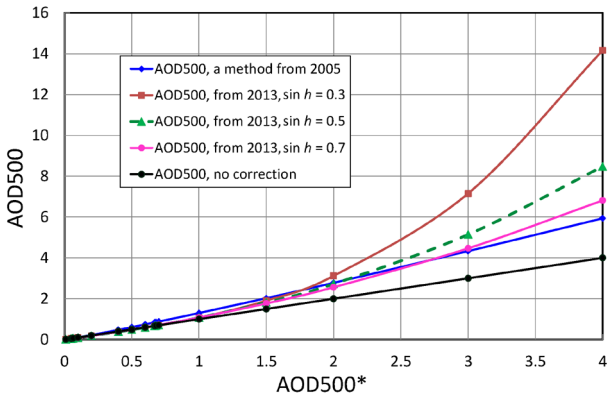

Fig. 1. Corrected aerosol optical depth at 500 nm (AOD500), by the method of Chubarova (2005) and by the method of Gorbarenko and Rublev (2013) for three different solar elevations, *h*, vs uncorrected AOD500*. The lowest curve, 1-to-1 line, is given for comparison.

The minimal turbidity, $\min AOD500^*$, where correction (6) has a sense, depends on the solar elevation:

$$\min \mathrm{AOD500}^* = 1.1 \times 0.5^{\frac{0.75\sin h + 0.125}{0.7}}, \tag{7}$$

e.g. for $\sin h = 0.3,\ 0.5,\ 0.7$, $\min AOD500^* = 0.78,\ 0.68,\ 0.58$, respectively. These values are definitely higher than $\min AOD500^* = 0.063$ for correction with formula (3) for M2b. The use of Eqs (2) and (6) together with condition (7) is denoted as model M2c.

Figure 1 compares results of correction with Eqs (3) and (6), in regard to their common input counterpart ($AOD500^* \ge 0$, including values even below the $\min AOD500^*$). Differences appear at very large turbidities and low sun. For $AOD500^* = 4$ the correction by Eq. (3), published in 2005, gives $AOD500 = 5.9$, but the new one by Eq. (6) from 2013 gives $AOD500 = 6.8$, 8.5, 14.2 for $\sin h = 0.7,\ 0.5,\ 0.3$, respectively.

2.5. Model G1

Apparently the most advanced broadband model was derived by Gueymard (1998), further denoted as G1. The model, originally for the prediction of AOD1000, contains about 30 formulas and allows varying several minor column gaseous components such as O_3 and tropospheric and stratospheric NO_2.

However, based on our evaluations and supported by Gueymard's error analysis (2013), the variability of the ozone amount can be considered a second-order input because of its small impact on the solar broadband direct beam. Besides, nitrogen dioxide would only be of concern over polluted areas. Therefore, in the extensive runs of Gueymard's model, we used the given fixed input values, typical for the Baltic Sea region: $O_3 = 0.35$ atm cm, NO_2(stratospheric) = 0.00012 atm cm,

NO_2(tropospheric) = 0.00004 atm cm, p = 1013.25 hPa (Kannel et al., 2012).

Concerning the Ångström wavelength exponent, in accordance with Gueymard, it is in general not possible to know a priori whether the observed aerosol particles belong to the continental, maritime, or any other specific type. Therefore, a fixed conventional value of $\alpha = 1.3$, representative of particles of rural-continental origin, was proposed by Gueymard.

The preliminary output for models M1 and M2 is originally AOD550, for G1 it is the Ångström turbidity coefficient, β = AOD1000. Transitions to AOD500 are easy applying the Ångström exponential formula in a general form:

$$\mathrm{AOD}(\lambda_2) = \mathrm{AOD}(\lambda_1)\left(\frac{\lambda_2}{\lambda_1}\right)^{-\alpha}. \quad (8)$$

2.6. Models T1 and T2

Two broadband models, T1 and T2, were developed at the University of Tartu. Model T1 is actually a modification of model M1 (Kannel et al., 2007), with some changes to consider the effects of circumsolar radiation (Kannel, 2007; Ohvril et al., 2009). The model is expressed by a single formula and has three input quantities: (1) Ångström exponent, α; (2) coefficient of column broadband transparency, p_2, transformed to atmospheric mass, $m = 2$; (3) precipitable water, W (Kannel, 2007; Kannel et al., 2007; Ohvril et al., 2009).

Model T2 was derived using barely a statistical approach. In creating the method, a large database, including almost 20 000 complex, spectral, and broadband direct solar beam observations at Tõravere, Estonia, during all seasons of an 8-year period 2002–2009, was used. Apparently, the model is local, and could be used only in conditions similar to Tõravere. Monthly climatology of column optical parameters for Tõravere will be given below in Section 6.

The model relies only on two input parameters: (1) coefficient of Bouguer column broadband transparency, p_2; and (2) precipitable water, W. These parameters allow calculating for $m = 2$ a specific quantity, the column broadband aerosol optical depth (BAOD2). According to Kannel et al. (2012), the two optical depth parameters, AOD500 and BAOD2, are strongly correlated ($R^2 = 0.96$) through a second-degree polynomial:

$$\mathrm{AOD500} = 1.7(\mathrm{BAOD2})^2 + 1.3(\mathrm{BAOD2}), \quad (9)$$

which enables an easy calculation of AOD500. Table 1 lists all considered broadband AODλ models with their input and output quantities.

3. OBSERVATIONAL DATA

We used two institutionally independent databases from the period 2002–2011.

1. Broadband direct solar irradiance and surface humidity measurements acquired at the Tartu–Tõravere Meteorological Station, Estonia. The station is included into the Baseline Surface Radiation Network (Kallis et al., 2005). The data allowed calculation of the coefficient of column transparency (p_2) and broadband aerosol optical depth (BAOD2) for each single observation. Note that the calculation of BAOD2 is not sensitive to uncertainties in precipitable water (W) estimations, thus W was estimated from the station surface water vapour pressure. Details of data processing are given in (Kannel et al., 2012). The quality of the W estimation is discussed in Section 6.
2. Spectral aerosol optical depth measurements by AERONET CIMEL photometers, which began regular observations in the territory of the meteorological station at Tõravere on 3 June 2002.

The two databases provided the opportunity to create a joint, integrated database for AODλ and broadband parameters of atmospheric transparency (turbidity). Our joint database includes 26 091 spectral-broadband solar direct irradiance and surface water vapour pressure observations for ten years, 2002–2011. About 75% of the observations were made in April, May, June, July, and August; 9% in September; 8% in March; 4% in October; and only 4% together in January, February, and November. In December no joint observations were made due to the low Sun and photometer calibrations.

The abundance of data enabled a comprehensive comparison of each model against the AERONET AOD500 observations.

4. TEST OF MODELS

Test runs of the eight models contained 26 091 single calculations of AOD500 by each model, followed by comparison against the reference AOD500(AERONET) value. Two models, M1 and T1, allow varying the input value of the Ångström exponent, α. For this reason additional runs were performed for these models with the variation of α.

To obtain quantitative measures on the accuracy of the models, we use two linear regression parameters, slope and correlation R^2 (actually coefficient of determination), and the following three commonly used statistical parameters (Iqbal, 1983; Gueymard, 1993):

(1) the mean bias deviation (MBD), expressing the average deviation (difference) of the predicted values, $y_i = \mathrm{AOD500(Model)}$, from the reference values, $x_i = \mathrm{AOD500(AERONET)}$:

$$\mathrm{MBD} = \frac{1}{N}\sum_{i=1}^{N}[y_i - x_i]; \qquad (10)$$

(2) the root mean square deviation (RMSD), a measure of the variation of predicted values around the reference values:

$$\mathrm{RMSD} = \frac{1}{N}\left[\sum_{i=1}^{N}(y_i - x_i)^2\right]^{1/2}; \qquad (11)$$

(3) the mean absolute relative deviation (MARD), also known as the mean absolute percentage deviation (MAPD), expressing the average value of relative deviations:

$$\mathrm{MARD} = \frac{1}{N}\sum_{i=1}^{N}\left|\frac{y_i - x_i}{x_i}\right|. \qquad (12)$$

The amount of column water vapour (W) is an input parameter to all considered AODλ models. It was estimated from surface conditions using correlation with vapour pressure, e_0 (Okulov et al., 2002). At the level of monthly means the used correlation performs quite well (Section 6), but for single observations the coefficient of determination, $R^2 = 0.83$, indicates a moderate scatter of $W(e_0)$ around $W(\mathrm{AERONET})$ (Kannel et al., 2012). Overestimation of W leads to underestimation of AODλ, even to a physically unrealistic negative AODλ. For the sake of brevity, sensibility analysis of the considered models to possible W errors is not included in the present paper. We only give the number of predicted negative AOD500 values together with the number of corrections applied for each run of the model (Table 2).

Results of the eight main runs are presented in Fig. 2, where each panel also reviews performance statistics of the run: slope, correlation R^2, number of corrected values and predicted negative values. Table 2 lists also results of six additional runs: (1) two runs for both M1 and T1 with a different fixed wavelength exponent, and (2) a run for both M1 and T1 with an a priori known wavelength exponent. The last two runs are visualized in Fig. 3.

From Table 2, which includes six statistics, one can rank the accuracy of the performance of the different models (with different Ångström α, if applied) in regard to different statistics. In summary, giving a point for the best result in each "event" of the "hexathlon", an overall, combined ranking for T2 appears to score 4 points, and for M2a, 2 points. These two models can be recommended, because of their consistently high performance in all items, for the evaluation of AOD500 in conditions similar to those at Tõravere. The two only models, M1 (row 4) and T1 (row 13), that consider a priori known Ångström exponents did not stand out. We try to analyse this disappointing result in the next two sections.

Table 2. Inputs of the Ångström exponent and performance statistics for AOD500 predictions by different models against AERONET observations during 2002–2011. In each run, the total number of predictions was 26 091. Numbers in bold indicate the best result in the column. Negative predictions are physically unrealistic

Row	Model, figure	Ångström α as input	Number of corrections	Performance statistics					
				Slope	R^2	Negative predictions	MBD	RMSD	MARD
1	M1	1.2	not used	0.935	0.933	107	−0.002	0.032	0.203
2	M1, Fig. 2	1.3	not used	0.974	0.936	129	0.003	0.030	0.214
3	M1	1.4	not used	1.016	0.938	143	0.009	0.031	0.233
4	M1, Fig. 3	individual	not used	1.055	0.945	159	0.013	0.032	0.247
5	M2, Fig. 2	1.0	not used	0.912	0.923	45	−0.004	0.034	0.203
6	M2a, Fig. 2	1.0	822	**0.995**	0.947	45	**0.001**	0.029	0.201
7	M2b, Fig. 2	1.0	21 733	1.060	0.947	45	0.011	0.033	0.230
8	M2c, Fig. 2	1.0	213	0.917	0.927	45	−0.004	0.033	0.203
9	G1, Fig. 2	1.3	not used	0.972	0.929	1	0.009	0.029	0.221
10	T1	1.2	not used	0.915	0.934	**0**	−0.003	0.032	0.197
11	T1, Fig. 2	1.3	not used	0.962	0.936	1	0.004	0.029	0.211
12	T1	1.4	not used	1.009	0.938	1	0.011	0.030	0.232
13	T1, Fig. 3	individual	not used	1.088	0.941	2	0.017	0.037	0.253
14	T2, Fig. 2	not used	not used	1.013	**0.957**	**0**	0.005	**0.026**	**0.188**

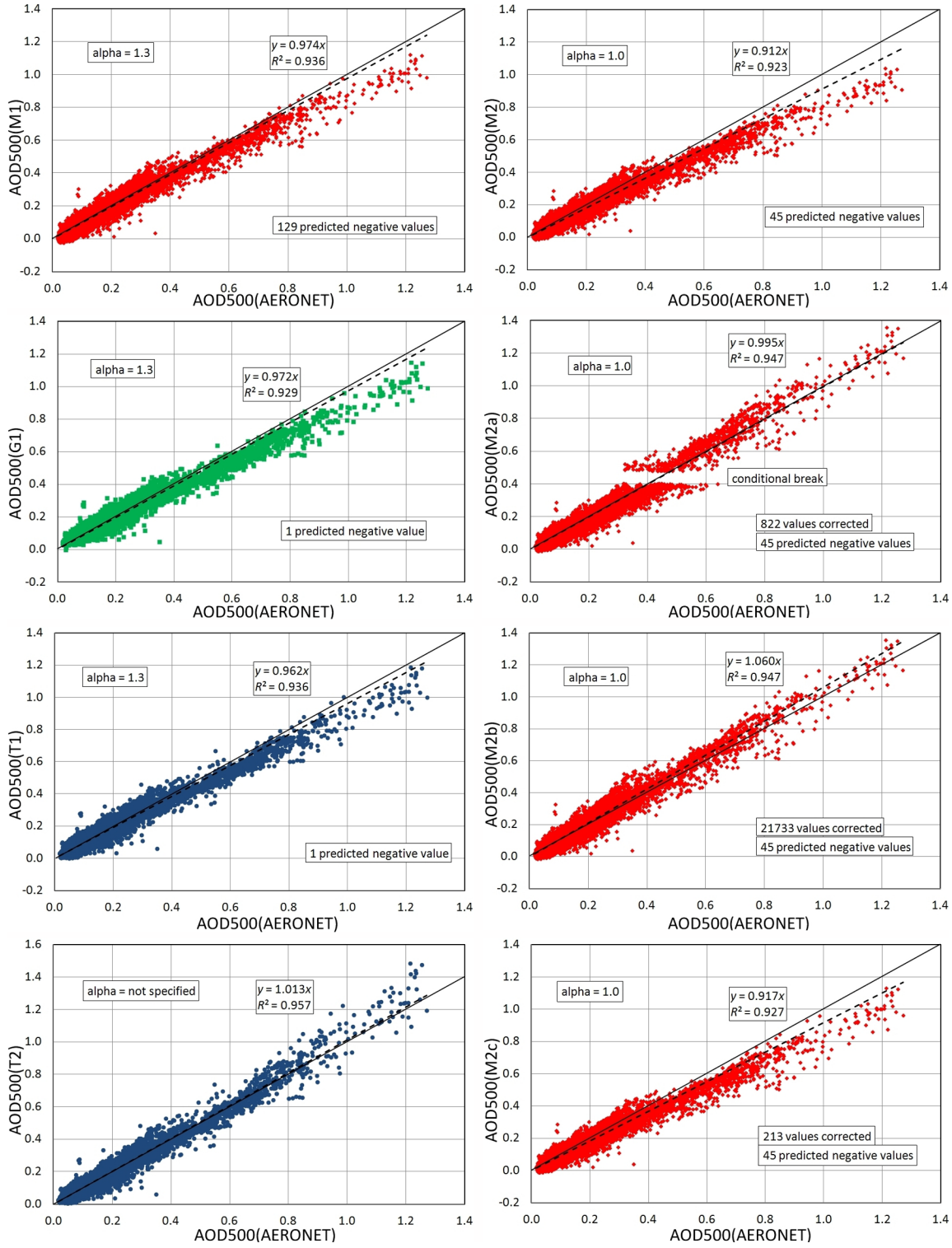

Fig. 2. Results of the main runs of different models: predicted AOD500 against the AERONET reference observations at Tõravere, Estonia. Each panel contains 26 091 single predictions for the years 2002–2011. All months, except December, are included. The Ångström exponent is fixed: $\alpha = 1$ or $\alpha = 1.3$. Models M2a, M2b, and M2c use each an individual correction scheme that improves predictions at greater turbidities. Dashed lines represent linear regression. Solid lines give 1-to-1 relationships.

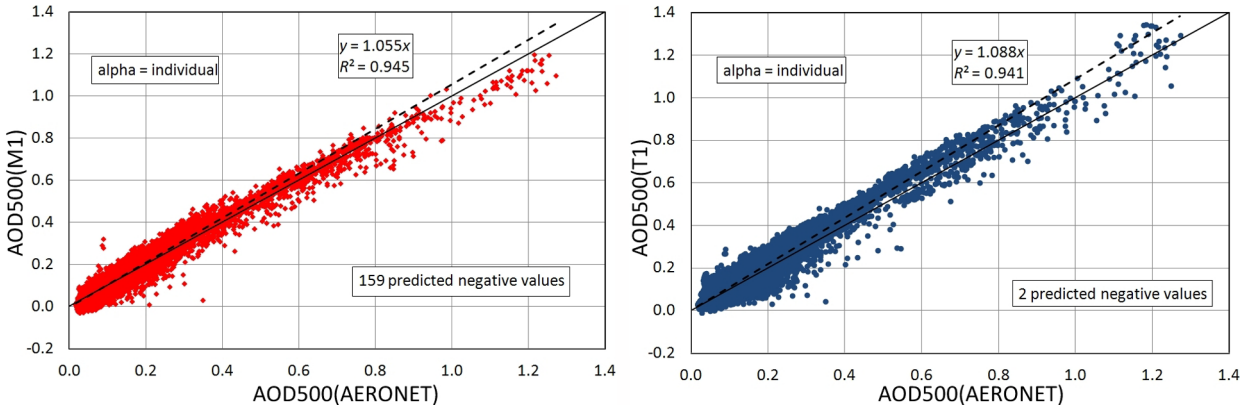

Fig. 3. Predicted AOD500 with M1 (left panel) and with T1 (right panel) against the AERONET observations at Tõravere, Estonia, 2002–2011. In each single prediction of total 26 091, the Ångström exponent is considered a priori known. Dashed lines represent linear regression. Solid lines give 1-to-1 relationships. Performance statistics of these runs (rows 4 and 13, Table 2) is not so convenient compared to runs of model M1 with appropriately fixed α or runs of T2 without the use of α.

5. FIXED VS INDIVIDUAL ÅNGSTRÖM EXPONENT

Usually broadband models for the calculation of AODλ do not enable changing the Ångström wavelength exponent, α. In this sense model M1 and its derivate, T1, represent an exception. Nevertheless, it is meaningful that the authors of model M1 themselves have actually not used this opportunity; they first began to use M2 and then M2a, in both of which the exponent is fixed, $\alpha = 1$. In model G1 the exponent is also fixed, $\alpha = 1.3$, but it assumes validity of the Ångström exponential formula (8). On the other hand, this means that the size distribution $n(r)$ is partly given by the Junge power law (Liou, 2002):

$$n(r) = C(r)\, r^{-(\alpha+3)}, \tag{13}$$

where C is a scaling factor proportional to particles column concentration and r is a particle radius. "Partly given" means that only the downgoing part of the size distribution (onward from the maximum) can be approximated by the power law.

Our joint 26 091 observation database is special, because each single observation contains also an Ångström AERONET-evaluated exponent, α(440-500-675–870), calculated as a best fit for the indicated four wavelengths. In this way the database enabled taking into consideration a priori known Ångström exponents for predicting single AOD500 values.

However, runs of models M1 and T1 with an a priori known α (rows 4 and 13, Table 2) did not give the expected improvement of the predictions (Fig. 3).

So, a priori known Ångström exponents did not improve AOD500 predictions. But should they? Consider the Ångström formula is obeyed, then the exponent enables only transition from a known $AOD\lambda_1$ to any other $AOD\lambda_2$, not to start with the magnitude of $AOD\lambda_1$ itself. In terms of the Ångström formula, prediction of $AOD\lambda_1$ can be done using a second parameter, the Ångström turbidity coefficient, β.

In the next section we examine the background, mainly seasonal variability of column optical and humidity properties at Tõravere, 2002–2011, and try to find regularities in the behaviour of the Ångström exponent.

6. VARIABILITY OF THE USED COLUMN OPTICAL AND HUMIDITY PARAMETERS

Figure 4 provides monthly means of the Ångström α and AOD500 and, in addition, seasonal variation of the fine mode fraction (FMF), which is one of the AERONET

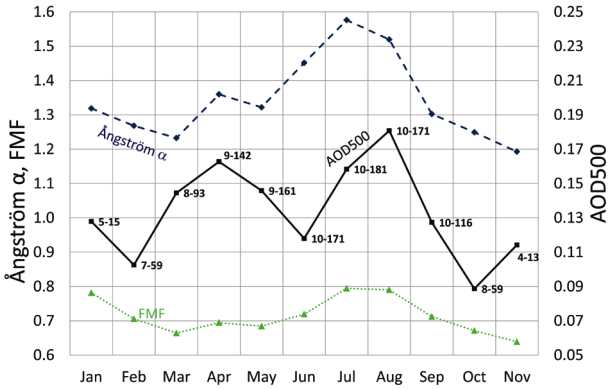

Fig. 4. Monthly means of the Ångström exponent, AOD500, and fine mode fraction (FMF) at Tõravere, Estonia. Labels give the total number of the respective months and days during 2002–2011 when the AERONET observations were performed: e.g. in January, the AERONET observations took place in 5 different years containing together 15 observational days.

inversion products describing the contribution of fine particles to AOD500. The AERONET inversion code finds the minimum of the size distribution within the radius interval from 0.439 to 0.992 μm. This minimum, approximately at 0.6 μm radius, is used as a separation point between fine and coarse mode particles. Using that separation, the inversion code calculates the contribution of fine particles to the formation of AOD500 (AERONET Inversion Products, 2010; O'Neill et al., 2001). The AERONET term, *fine particles*, actually includes three traditional subregions of aerosol size distribution: the nucleation, Aitken, and accumulation mode.

As expected, the intra-annual evolution of the Ångström exponent is consistent with monthly changes in the FMF. The higher values in summer (Jun–Jul–Aug) indicate domination of fine aerosol particles.

Somewhat surprising is a local minimum of AOD500 in June. For the cold season, we have no good explanations to the higher AOD500 in January and November compared to February and October; this is a topic of further studies.

The monthly means of column transparency (p_2) for 2002–2011 (Fig. 5) are in opposite phase with AOD500, with an expected local maximum in June. Actually, higher column transparency in June was noticed already since 1994. This finding can be explained by a general cleaning of the European atmosphere as a part of the global brightening (Ohvril et al., 2009; Okulov and Ohvril, 2010). During June, the Estonian landscape is already totally covered with fresh vegetation, which restricts creation and vertical distribution of dust. The number of forest and bog fires is also low in June.

Column precipitable water (W) is usually evaluated from surface humidity and temperature, in our study:

$$W(\text{mm}) = 1.48e_0 + 0.40, \qquad (14)$$

where e_0 (mb) is the 12 UTC surface water vapour pressure. This parameterization was developed from clear-sky radio soundings in Tallinn (Okulov et al., 2002). For Tõravere, Kannel et al. (2012) compared column humidity predictions, $W(e_0)$, with W(AERONET), where the latter were considered as reference. Use of almost 20 000 parallel observations from 2002–2009 showed that the prediction overestimates the reference as an average only by 3%. For monthly means of W over all considered years (2002–2011), approximation (14) gives values close to those obtained by the AERONET photometer (Fig. 6).

To model the extinction of broadband direct solar beam, for optical mass $m = 2$, we assume that the atmosphere consists of three layers or substances (Kannel et al., 2012): an ideal or clean and dry atmosphere (CDA), integrated column water vapour (W), and atmospheric aerosol particles.

Figure 7 shows monthly mean broadband transmittances for these three layers at Tõravere, calculated from our database for a 10-year period, 2002–2011. The plots were prepared using only meteorological data, not the AERONET observations. Noticeable is the summer maximum of aerosol broadband transmittance in June, which apparently is the main reason of higher total column transmittance in this month. The lowest total transmittance occurs in July and August, caused by low transmittances of both column water vapour and aerosols.

Figure 8 shows the seasonal variation of total broadband optical depth, and its division into the main atmospheric constituents.

Unfortunately, the annual cycles of the reviewed column parameters (except the fine mode fraction) do not give us the expected relationships with the annual cycle of the Ångström exponent (Fig. 4). Moreover, a plot of the Ångström α against AOD500 revealed no correlation (Fig. 9). The α varies from 0.05 to 3.43 for cleaner air, when AOD500 < 0.2 encompassing the

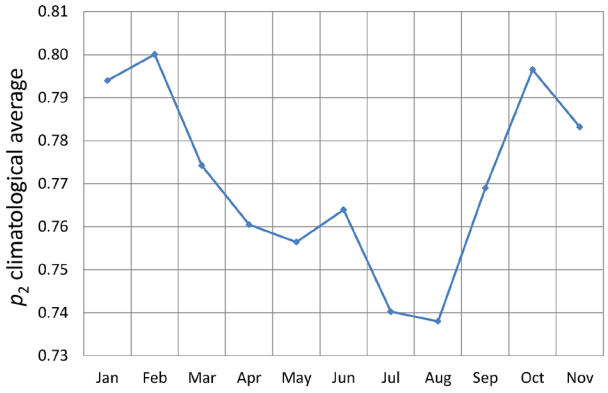

Fig. 5. Monthly means of the atmospheric integral transparency coefficient p_2 at Tõravere, Estonia, 2002–2011. The database included no observations in December.

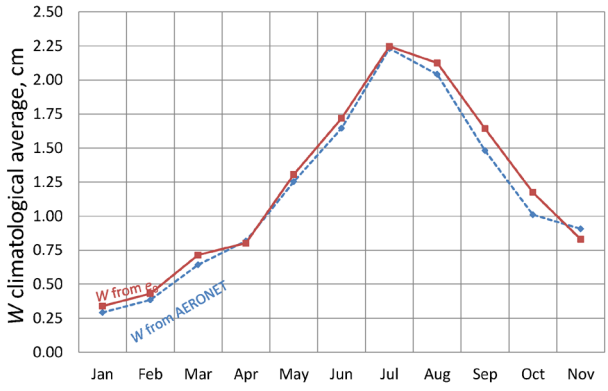

Fig. 6. Monthly mean precipitable water at Tõravere, Estonia, 2002–2011. The solid line corresponds to estimations through surface water vapour pressure, $W(e_0)$. The dashed line represents AERONET photometric observations, W(AERONET).

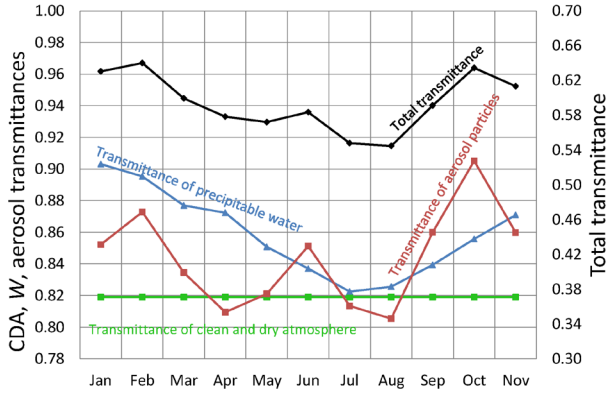

Fig. 7. Broadband transmittances, for a slant column, $m = 2$ (solar elevation $h \approx 30°$) of different atmospheric layers at Tõravere, Estonia, 2002–2011. Calculations are based solely on meteorological and broadband actinometric observations, not the AERONET spectral observations. Total transmittance is scaled to the secondary vertical axis.

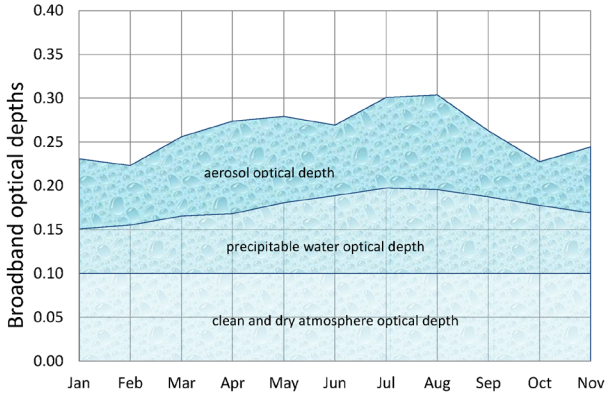

Fig. 8. Broadband optical depths for atmospheric layers at Tõravere, Estonia, 2002–2011. Calculations for a slant column, $m = 2$ (solar elevation $h \approx 30°$). Monthly mean values are affiliated to beginnings of months.

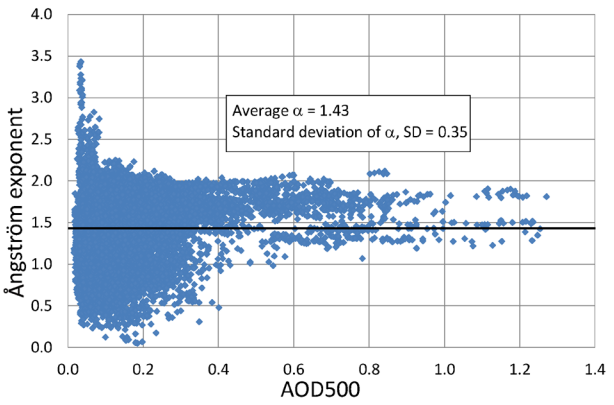

Fig. 9. Ångström exponent plotted against AOD500 at Tõravere, 2002–2011. Number of observations 26 091.

simple (nonclimatological) average of the exponent, $\alpha = 1.43$. The standard deviation (one sigma uncertainty) of the exponent for the whole database $\sigma = 0.35$.

Supposing normal distribution and coverage factor 3, the expanded 3σ-uncertainty becomes 1.05. Compared to the average value of our database, $\alpha = 1.43$, or the conventional value, $\alpha = 1.3$, the irregularity of the Ångström exponent is really noteworthy. For high turbidities, AOD500 > 0.85, the scatter of α is smaller, $1.2 < \alpha < 1.9$.

To conclude, Fig. 9 is a visual argument about the lack of relationship between the Ångström α and AOD500. Atmospheric aerosol particles, apparently, represent a composite of several different types and sizes, which means that the relationship between $\ln(\mathrm{AOD}\lambda)$ and $\ln(\lambda/\lambda_0)$ is more complicated than a linear one. The Ångström exponent is not correlating with AODλ and, thus, including it into the AODλ broadband models does not improve the predictions.

7. CONCLUSIONS

Eight broadband models have been selected for investigation of their accuracies to predict aerosol spectral optical depth, AOD500. Seven of the considered models were simple ones, expressed with some formulas only. Such a simplistic approach is often sufficient for the interpretation of long-term changes in the column aerosol content, description of radiation regime, modelling of radiative transfer, validation of aerosol impact in climatological models, correction of satellite imagery, etc.

Broadband direct solar irradiance, as an input parameter to the models, was observed at the Tartu-Tõravere Meteorological Station (Estonia), which is included in the Baseline Surface Radiation Network. Precipitable water (W) was derived from surface water vapour pressure. All models were tested against AOD500 reference values obtained by the AERONET Cimel photometer located at the same station.

Even a visual review (Fig. 2) demonstrates that for relatively clean air, AOD500 < 0.6, all considered broadband models give reasonable results. For more turbid air, AOD500 > 0.6, the models (if not corrected) tend to underestimate the aerosol optical depth. The underestimation is inherent only in physical (i.e. non-statistical) models. The main reason for the underestimation of AODλ at higher turbidities is that models consider only a narrow solar direct beam, exactly from the solar disc with its mean angular diameter of about 32′.

Analysis of turbidity data from the smoky summers of 2002 and 2010 in Moscow led to a necessity to increase physically predicted AOD500 values using a

statistical approach. Three different correction schemes were proposed.

Results of the test runs (Table 2) showed that two models, T2 and M2a, performed better compared to others. Model T2 scored best in three statistics without any negative AOD500 predictions. Model M2a was best in two statistics, but gave 45 negative predictions. It should be noted that model M2a has an artificial limitation: predicted values between $0.4 < \mathrm{AOD500} < 0.477$ are not applicable. In summary of intercomparison, these two models can be recommended for proxy calculation of AOD500.

Two considered models, M1 and T1, enable input of an a priori known Ångström wavelength exponent α for each single prediction, but with no improvement of performance. In order to find reasons for this failed numerical experiment, we analysed climatological variability of column optical and humidity parameters in terms of monthly means at Tõravere during 2002–2011. Correlation with the coefficient α was established only with the fine mode fraction (FMF).

A study of the annual courses of column optical parameters revealed an interesting fact: a spring–summer maximum of atmospheric column transparency in June. This finding was supported by low values of both broadband aerosol optical depth and AOD500. Cleaner air in June can be explained by (1) fresh vegetation, which restricts generation of dust, and (2) low number of forest and bog fires in Estonia as well as in its surrounding areas.

ACKNOWLEDGEMENTS

This investigation was supported by the project "Estonian Radiation Climate" funded by the European Regional Development Fund and by the Estonian Research Council through project TFP SF0180038s08. The authors would like to thank anonymous referees for their commitment and relevant comments.

REFERENCES

Abakumova, G. M. and Gorbarenko, E. V. 2008. *Atmospheric Transparency in Moscow During the Last 50 Years and Its Variability on the Russian Territory*. LKI Publishing (in Russian).

AERONET Inversion Products, 2010. http://aeronet.gsfc.nasa.gov/new_web/Documents/Inversion_products_V2.pdf (accessed 10.10.2013).

Carlund, T., Landelius, T., and Josefsson, W. 2003. Comparison and uncertainty of aerosol optical depth estimates derived from spectral and broadband measurements. *J. Appl. Meteor.*, **42**, 1598–1610.

Chubarova, N. E. 2005. Optical and radiative properties of smoke aerosol from AERONET data. In *Handbook of Moscow Environmental and Climatic Features. Vol. 1. Applied Climatic Parameters, Air Pollution Monitoring, Dangerous Weather Phenomena, Expected Tendencies in the XXI Century*, pp. 127–132. Geography Department of MSU (in Russian).

Chubarova, N. E., Gorbarenko, E. V., Nezval′, E. I., and Shilovtseva, O. A. 2011a. Aerosol and radiation characteristics of the atmosphere during forest and peat fires in 1972, 2002 and 2010 in the Region of Moscow. *Izvestiya RAN. Fizika Atmosfery i Okeana*, **47**(6), 790–800 (in Russian).

Chubarova, N. E., Gorbarenko, E. V., Nezval′, E. I., and Shilovtseva, O. A. 2011b. Aerosol and radiation characteristics of the atmosphere during forest and peat fires in 1972, 2002 and 2010 in the Region of Moscow. *Izvestiya, Atmospheric and Oceanic Physics*, **47**(6), 729–738. Pleiades Publishing, Ltd (translation from Russian).

Garg, H. P. and Prakash, J. 2006. *Solar Energy. Fundamentals and Applications*. Tata McGraw-Hill Publishing Company Limited, New Delhi.

Gorbarenko, E. V. and Rublev, A. N. 2013. Correction of aerosol optical thickness succession under strong atmospheric turbidity. In *Proceedings of International Symposium "Atmospheric Radiation and Dynamics" (ISARD-2013), 24–27 June 2013, Saint-Petersburg, Saint-Petersburg State University*, p. 105.

Gueymard, C. 1993. Critical analysis and performance assessment of clear sky solar irradiance models using theoretical and measured data. *Solar Energy*, **51**(2), 121–138.

Gueymard, C. 1998. Turbidity determination from broadband irradiance measurements: a detailed multicoefficient approach. *J. Appl. Meteor.*, **37**, 414–435.

Gueymard, C. 2013. Aerosol turbidity derivation from broadband irradiance measurements: methodological advances and uncertainty analysis. In *Solar 2013 Conference. Baltimore, MD*. American Solar Energy Society.

Holben, B., Eck, T. F., Slutsker, I. Tanré, D., Buis, J. P., Setzer, A. et al. 1998. AERONET – a federated instrument network and data archive for aerosol characterization. *Remote Sens. Environ.*, **66**, 1–16.

Iqbal, M. 1983. *An Introduction to Solar Radiation*. Academic Press.

Kallis, A., Russak, V., and Ohvril, H. 2005. 100 years of solar radiation measurements in Estonia. In *Report of the 8th Session of the Baseline Surface Radiation Network (BSRN) Workshop and Scientific Review, Exeter, UK, 26–30 July 2004*, pp. C1–C4. World Climate Research Programme, WMO, WCRP Informal Report No. 4/2005, March 2005.

Kannel, M. 2007. Atmosfääriaerosooli spektraalse optilise paksuse modelleerimine. Master thesis. University of Tartu, Estonia.

Kannel, M., Ohvril, H., Teral, H., Russak, V., and Kallis, A. 2007. A simple broadband parameterization of columnar aerosol optical thickness. *Proc. Estonian Acad. Sci. Biol. Ecol.*, **56**, 57–68.

Kannel, M., Ohvril, H., and Okulov, O. 2012. A shortcut from broadband to spectral aerosol optical depth. *Proc. Estonian Acad. Sci.*, **61**, 266–278.

Lenoble, J. 1993. *Atmospheric Radiative Transfer*. A. Deepak, Hampton, Virginia, USA.

Liou, K. N. 2002. *An Introduction to Atmospheric Radiation*. Academic Press.

Okulov, O. and Ohvril, H. 2010. *Column Transparency and Precipitable Water in Estonia. Variability During the Last Decades*. Lambert Acad. Publ., Saarbrücken, Germany.

Okulov, O., Ohvril, H., and Kivi, R. 2002. Atmospheric precipitable water in Estonia, 1990–2001. *Boreal Environ. Res.*, **7**, 291–300.

Ohvril, H., Okulov, O., Teral, H., and Teral, K. 1999. The atmospheric integral transparency coefficient and the Forbes effect. *Solar Energy*, **66**(4), 305–317.

Ohvril, H., Teral, H., Neiman, L., Kannel, M., Uustare, M., Tee, M., et al. 2009. Global dimming and brightening versus atmospheric column transparency, Europe, 1906–2007. *J. Geophys. Res.*, **114**, 1–17.

O'Neill, N. T., Eck, T. F., Holben, B. N., Smirnov, A., Dubovik, O., and Royer, A. 2001. Bimodal size distribution influences on the variation of Angström derivatives in spectral and optical depth space. *JGR*, **106**(D9), 9787–9806.

Tarasova, T. A. and Yarkho, E. V. 1991a. Determination of atmospheric aerosol optical thickness from land-based measurements of integral direct solar radiation. *Meteorologiya i gidrologiya*, 12, 66–70 (in Russian).

Tarasova, T. A. and Yarkho, E. V. 1991b. Determination of atmospheric aerosol optical thickness from land-based measurements of integral direct solar radiation. In *Soviet Meteorology and Hydrology*, 12, pp. 53–58. Alerton Press, New York (translation from Russian).

Toledano, C., Cachorro, V. E., Sorribas, M., Berjón, A., Morena de la, B. A., Frutos de, A. M., and Gouloub, P. 2007. Aerosol optical depth and Ångström exponent climatology at El Arenosillo AERONET site (Huelva, Spain). *Quart. J. Roy. Meteor. Soc.*, **133**, 795–807.

Aerosooli spektraalse optilise paksuse arvutusmudelite võrdlus ja kontroll AERONET-i mõõtmistega

Martin Kannel, Hanno Ohvril, Oleg Okulov, Kaidi Kattai ja Lennart Neiman

Artiklis on omavaheliseks võrdluseks valitud seitse lihtsat ja üks keerukam aerosooli spektraalse optilise paksuse (AOD500) arvutamise integraalset ehk laiaribalist mudelit. Lihtsad mudelid koosnevad vaid mõnest valemist ja vajavad ainult kaht peamist sisendparameetrit, milleks on Päikese integraalse otsekiirguse kiiritustihedus koos Päikese kõrgusega või atmosfäärisamba läbipaistvuskoefitsient ning atmosfääri veeaurusisaldus. Mudelites pole tehtud eeldusi aerosooliosakeste füüsikaliste omaduste kohta, kuid kaks mudelit (M1 ja T1) lubavad kolmanda sisendparameetrina varieerida Ångströmi lainepikkuse eksponenti α, mis on seotud osakeste suurusjaotusega.

Ainus analüüsitud keerukam mudel (G1) koosneb umbes 30 valemist ja lubab spetsifitseerida atmosfääri gaasilist koostist detailsemalt, näiteks osooni- ning lämmastikdioksiidikoguste kaudu.

AOD500 arvutused toetusid Tõraveres mõõdetud Päikese laiaribalisele otsekiirguse kiiritustihedusele, mille mõõteandmeid võib kvaliteetseteks pidada, sest Tartu-Tõravere ilmajaam kuulub rahvusvahelisse kiirgusmõõtmiste võrgustikku BSRN. Teine sisendsuurus, õhusamba veeaurusisaldus, ei olnud otseselt mõõdetud, vaid leitud kaudselt, veeaururõhu kaudu. Kõigi mudelite saadud AOD500 tulemusi võrdlesime AOD500 tegelike väärtustega, mõõdetuna Tõraveres AERONET Cimel-i fotomeetri poolt.

Mudelite võimekuse analüüsiks koostasime ulatusliku andmebaasi, milles iga vaatlusrida ühendas nii ilmajaamas mõõdetud suurused (Päikese integraalne otsekiirgus, veeaururõhk) kui ka AERONET-i fotomeetri samaaegselt mõõdetud suurused (AOD500 tegelik väärtus, Ångströmi lainepikkuse eksponent, α(440-500-675–870)). Kokku sisaldas andmebaas 26 091 integraalset-spektraalset vaatlust, mis toimusid kõikidel kalendrikuudel (välja arvatud detsember) kümne aasta jooksul, 2002–2011. Selline andmebaas võimaldas iga mudeli põhjalikku võrdlust AERONET-i tegelike AOD500 mõõtmistega.

Suhteliselt puhta õhu korral, AOD500 < 0,6, andsid kõik mudelid mõistlikke tulemusi. Saastatuma õhu korral, mil AOD500 > 0,6, kaldusid statistiliselt korrigeerimata mudelid aerosooli optilist paksust alahindama. Alahindamist põhjustab Päikese oreooli nn parasiitkiirgus, mis suurendab aktinomeetri mõõdetud otsekiirgust ja loob mulje puhtamast õhust.

Testimistulemused tõstsid esile kaks mudelit: T2 ja M2a. Tuleb siiski märkida, et mudeli M2a väljundis on kunstlik piirang, puuduvad arvutatud väärtused vahemikus 0,4 < AOD500 < 0,477. Vaatlusalustest mudelitest kaks, M1 ja T1, võimaldasid sisendsuurusena muuta ka Ångströmi lainepikkuse eksponenti α. Tavapraktikas pole α-väärtused *a priori* teada, koostatud andmebaasis aga sisaldus selline võimalus. Mõnevõrra ootamatult ei parandanud α kaasamine AOD500 arvutustulemusi. Leidmaks põhjusi selle ebaõnnestunud numbrilise eksperimendi kohta, analüüsisime atmosfäärisamba optiliste ja niiskusparameetrite sesoonset muutlikkust Tõraveres aastatel 2002–2011. Selgus, et Ångströmi α korreleerub vaid osakeste nn peenmoodi fraktsiooni (FMF) panusega AOD500-sse. Kuu

keskmiste lõikes näitas FMF head korrelatsiooni Ångströmi eksponendiga ja peenosakeste domineerimist suvekuudel.

Kõrvalproduktina AOD500 mudelite võrdlemisele selgus, et atmosfääri läbipaistvusel on juunis kevadsuvine maksimum, põhjuseks ilmselt õhusamba väiksem aerosooliosakeste sisaldus. Esialgu oskame seda fakti põhjendada arvamusega, et juunis on Eestis välja kujunenud värske taimkate, mis takistab tolmu teket ja levikut. Samuti pole juunis veel levinud kohalikud raba- ja metsapõlengud.

Uuringut toetasid kaks projekti: Euroopa regionaalarengu fondi rahastatav “Eesti kiirguskliima” ja Eesti Teadusnõukogu sihiteema TFP SF0180038s08.